Journal of Materials Processing Tech. 322 (2023) 118214

Contents lists available at ScienceDirect

Journal of Materials Processing Tech.

journal homepage: www.elsevier.com/locate/jmatprotec

A new flexible multi-point incremental sheet forming process with multi-layer sheets

Xuelei Zhao *, Hengan Ou *

Department of Mechanical, Materials and Manufacturing Engineering, Faculty of Engineering, University of Nottingham, NG7 2RD, UK

ARTICLE INFO

Associate Editor: Marion Merklein

Keywords:
Incremental sheet forming
Flexible multi-point sheet forming
Sheet thinning
Wrinkling
Formability

ABSTRACT

In this research, a new flexible multi-point incremental sheet forming process with multi-layer sheets (F-MPIF-MLS) was proposed. The novelty of this new forming process is demonstrated by two specific aspects of contribution. The first is the development of a new flexible multi-point die system to replace the conventional multi-point die, in which the multi-point pins are in contact with and provide support to the blank sheet from the start to the end of the forming operation. The second is the use of multi-layer sheets, which allows the target blank sheet to be deformed without clamping constraints. The new F-MPIF-MLS process clearly shows the benefits of overcoming the limitations of excessive sheet thinning and poor surface finish of the existing conventional multi-point incremental sheet forming (MPIF) process. A detailed comparative investigation into the new F-MPIF-MLS and the conventional MPIF processes is conducted through experimental testing and finite element (FE) simulation. The results show a noticeable reduction of wrinkling by using the new flexible multi-point die over the conventional multi-point die system with multi-layer sheets to form a dome shape. Moreover, in using the new F-MPIF-MLS process, the maximum thickness reduction is significantly reduced from 35% to 5% as compared to the conventional MPIF process to achieve a more uniform thickness distribution of the formed part.

1. Introduction

The need for manufacturing small batches or customised products requires the development of innovative flexible sheet forming processes. Incremental sheet forming (ISF) is a flexible sheet forming process that has drawn significant attention in the past two decades. The core concept of the ISF process is to use a hemispheric forming tool moving along a predefined tool path to deform the blank sheet into a designed product through localised deformation of the blank sheet. The motion of the forming tool is controlled by a computer numerical controlled (CNC) milling machine (Jeswiet et al., 2005; Duflou et al., 2018). Common types of ISF processes can be generally classified into single-point incremental sheet forming (SPIF), two-point incremental sheet forming (TPIF), and double-sided incremental sheet forming (DSIF) processes (Kumar et al., 2019). The SPIF process may be characterised by the motion of a hemispheric tool that has a single-point contact with the blank sheet. The blank sheet is clamped by a blank holder, as presented in Fig. 1(a). The DSIF process is a variant of the ISF process, where a support tool is used at the opposite side of the blank sheet and follows the motion of the forming tool during the incremental forming process (Peng et al., 2019), as presented in Fig. 1(b). The additional compression due to the support tool in the DSIF process presents benefits for improved formability. At the same time, a more sophisticated multi-axis CNC machine and ISF tool path strategy for DSIF processing are required (Peng and Ou, 2023). In contrast to the SPIF process, the TPIF process involves the use of a partial or full die to support the blank sheet during the same incremental deformation process (Attanasio et al., 2008), as shown in Fig. 1(c) and (d), respectively. In the TPIF process with a full die, the full die provides full support to the blank sheet and enhances the geometrical accuracy, but each full die has to be bespoke for a specific product. In the TPIF with a partial die, the partial die only supports part of the blank sheet. It is difficult to modify the tool path and die geometry in the TPIF process with a full die to correct geometrical errors. Thus, a partial die offers more flexibility than a full die in the TPIF process (Silva and Martins, 2013).

Although the use of a supporting die may lead to a reduction in forming flexibility and an increase in cost and lead time, recent research suggests that the TPIF process has advantages over the SPIF process in a

* Corresponding authors.
E-mail addresses: Xuelei.Z@outlook.com (X. Zhao), h.ou@nottingham.ac.uk (H. Ou).

https://doi.org/10.1016/j.jmatprotec.2023.118214
Received 31 July 2023; Received in revised form 3 November 2023; Accepted 11 November 2023
Available online 16 November 2023

number of ways. Lasunon and Knight (2007) conducted FE simulations and experimental testing to compare the SPIF and TPIF processes by producing a pyramidal part. The authors found that maximum thinning was observed on the sidewall in the TPIF, while it occurred in the corner in the deformed part by SPIF process. The TPIF process could produce a more uniform thickness distribution than the SPIF process. And a part with a sharp edge can be easily formed by the TPIF process. An analytical model was developed and validated experimentally by Silva and Martins (2013) to compare the formability between the SPIF process and the TPIF process with a partial die. Both predicted and measured results showed that better geometrical accuracy could be obtained by the TPIF with a partial die as compared to the SPIF process because of the smaller amount of elastic recovery upon unloading, i.e., less springback achieved by the TPIF process. Similar findings were reported by Bagudanch et al. (2017) in producing a customised cranial implant with an ultrahigh molecular weight polyethene sheet. The authors found that the maximum dimensional deviation obtained from the SPIF process was 7 mm before the trimming operation, while this value could be reduced to 4.5 mm by using the TPIF process. Furthermore, the use of a supporting die can effectively reduce the pillow effect that is observed in the SPIF process and then enhance the geometrical accuracy (Reddy et al., 2015). The first observations on the pillow effect were reported by Ambrogio et al. (2007). The authors explained that the pillow effect resulted from overbending, which tended to increase the bending at the opening region, especially in the flat region of the parts deformed by the SPIF process. Nevertheless, due to the use of dies to support the flat area, no notable pillow effect was observed in the TPIF process deformed part, as demonstrated by Lu et al. (2017). Compared to the SPIF process, the TPIF process can result in better geometrical accuracy. To improve the flexibility of the TPIF process, a reconfigurable multi-point die has been used to replace the conventional full or partial die.

Nakajima (1969) was first to develop the reconfigurable multi-point die, which used a group of pins to replace conventional solid dies. The length of each pin in a multi-point die could be varied independently to build a complicated three-dimensional (3D) surface (von Finckenstein, 1995). Dimpling, wrinkling, and springback are the three typical defects in the multi-point forming process (Cai et al., 2008). When employing a multi-point die, the total contact area of the multi-point pins is much smaller than that of the blank sheet. Therefore, the contact region between the blank sheet and the multi-point die is discontinuous, so dimples can easily occur. An efficient and common way to suppress dimples was to place a piece of polymer sheet between the multi-point die and the blank sheet. However, the hyperelastic polymer sheet deformation is inhomogeneous, which leads to uneven stress and strain distribution on the blank sheet. A novel hybrid steel and polyurethane pad was proposed by Erhu et al. (2018) to effectively disperse the concentrated load caused by multi-point units and result in better strain distribution than the use of a polyurethane pad. Wrinkling is caused by compressive instability under the action of external force. Li et al. (2007) developed a multi-point forming with varying paths. The shape of the multi-point die was varied continuously, and all the multi-point pins could keep in contact with the blank sheet during the whole process. Compressive instability could result from excessively high local in-plane compressive stress. As a result, the strain and stress distributions became more homogenous, and wrinkling was eliminated. In addition, Liu et al. (2017) developed a new flexible blank holder that could be used to adjust the blank holder force. Because the stress state in the blank sheet could be affected by the blank holder force, more uniform stress distribution would be obtained after applying this new design without wrinkling. Springback normally occurs when the forming loads are removed, e.g., by removing the punch or lifting the blank holder, leading to dimensional inaccuracies. An algorithm for springback compensation in the multi-point forming process was established by Zhang et al. (2013), which was verified by producing several curved surfaces. The authors reported good agreement between the predicted and experimental results, and the results matched the target profiles and met the precision requirements.

The concept of using a multi-point die in the ISF process was first reported by Li et al. (2009) and is regarded as the multi-point incremental sheet forming (MPIF) process. Except for the multi-point

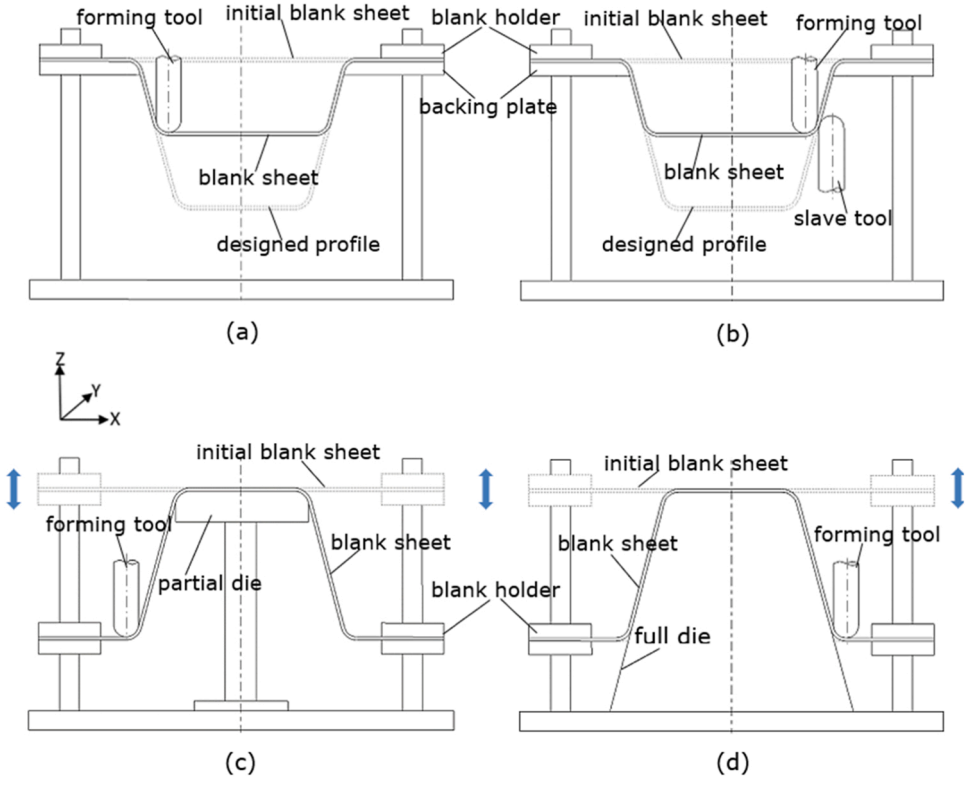

Fig. 1. Four common types of the ISF processes: (a) SPIF, (b) DSIF, (c) TPIF with partial die, (d) TPIF with full die.

supporting die, the basic components in the MPIF process are similar to the TPIF process. The multi-point pins used in this case were placed in fixed positions. Each multi-point pin should be adjusted to the desired position before the forming operation. During the forming process, the forming tool moved along the designed tool path, and the blank sheet was clamped by the blank holders and then moved downward together. The movement of the blank sheet and blank holder should be the same as the tool path of the forming tool in the vertical direction. Compared to the conventional TPIF process, the MPIF process could not only increase the flexibility of the process but also decrease the cost and shorten the forming lead time. Boudhaouia et al. (2018) indicated that the material deformation in the MPIF process was quite similar to that of the TPIF process. Nourmohammadi et al. (2019) conducted FE simulations and experimental testing to compare the MPIF and TPIF processes. The results showed that the distributions of thickness and equivalent plastic strain were in good agreement between the parts formed by the TPIF and MPIF processes. However, dimples may easily occur in the MPIF produced parts due to the discontinuous contact between the multi-point die and blank sheet. As a result, the MPIF process leads to lower geometrical accuracy and poorer surface finish than the TPIF process. Moreover, Nourmohammadi et al. (2019) compared the MPIF processes with a full and partial die by creating a part with compound curvature. The authors found that using a full die in the MPIF process could induce higher plastic strain, which increased the possibility of fracture compared to a partial die. In this case, the multi-point partial die could obtain higher formability. In addition to the MPIF process, Lu et al. (2014) and Zhang et al. (2017) developed a hybrid ISF process by combining the multi-point forming and the ISF processes sequentially. The forming operation was completed through two separate forming methods, i.e., stretch forming by using multi-point die and SPIF processes. The reconfigurable multi-point die was only applied in the first stage of stretch forming. Since the edge of the target blank sheet was not fully constrained, more material was allowed to flow into the deformation region during the multi-point stretch forming stage. As a result, with the material supplement, the sheet thinning was significantly reduced, and higher formability would be achieved as compared to the conventional ISF process.

Apart from the aforementioned hybrid ISF processes, researchers developed new ISF processes for enhanced formability. A three-sheet incremental sheet forming process was proposed by Chang and Chen (2020). The target blank sheet was placed between the upper and lower dummy sheets when conducting the SPIF process. The upper dummy sheet was used to avoid the forming tool in direct contact with the target blank sheet so that the surface quality can be improved. The lower dummy sheet offered additional compressive stress to the target blank sheet to achieve decreased stress triaxiality on the deformed part, which could delay crack growth. Nevertheless, it could be found that the basic mechanism of sheet deformation in the three-sheet ISF process was the same as the conventional SPIF process. Based on the three-sheet incremental sheet forming process, Chang and Chen (2022) developed the flexible free ISF process to produce low ductile materials (e.g., magnesium and titanium alloys) at room temperature. The difference from the above three-sheet incremental sheet forming process was that the target blank sheet was deformed without any edge constraint in the flexible free ISF process. At the same time, the target blank sheet was trimmed into the designed profile before the ISF process. The results showed that the flexible free ISF process could produce a part with less thinning, more uniform thickness distribution, and better geometrical accuracy than the conventional SPIF process. Xu et al. (2023) developed a three-layer two-point incremental sheet forming process to produce a woven fabric composite sheet. The woven fabric composite sheet was placed between the upper and lower metal dummy sheets. Notably, akin to the flexible free ISF process, this approach enabled the production of the desired fabric sheet without the imposition of edge constraints. The authors indicated that edge slippage and in-plane shear were the principal deformation behaviours in the proposed forming process.

Although current hybrid ISF processes have successfully addressed some existing limitations, there are plenty of opportunities for further advances in developing new hybrid ISF processes. The use of a multi-point die in the current ISF processes can only improve process flexibility and save the associated cost of tooling. However, material deformation in the implementation of a multi-point die is identical to that of using a conventional rigid die. Low geometrical accuracy, sheet thinning, and dimpling defects are still limiting factors in the development of the MPIF process. In this research, a new flexible MPIF process is developed. This new flexible MPIF process is different from the current MPIF process, in which each pin keeps contact with the blank sheet during the whole forming process. Using this concept, the new flexible MPIF process can be carried out with single- or multi-layer sheets. When using the multi-layer sheets, the target blank sheet is expected to be deformed without edge constraints to reduce sheet thinning and achieve uniform deformation.

The basic concept of the new flexible MPIF process and its variations are discussed in Section 2. The proposed new flexible MPIF process with multi-layer sheet (F-MPIF-MLS) was demonstrated through experimental testing and finite element (FE) simulation. The experimental setup and FE modelling are presented in Sections 3 and 4, respectively. Section 5 discusses the measured and predicted results with particular attention given to the three sets of comparisons: the conventional MPIF and new flexible MPIF processes, the conventional MPIF process with multi-layer sheets and the new flexible MPIF processes with multi-layer sheets, and the conventional MPIF process and the new flexible MPIF process with multi-layer sheets. The findings are presented in the conclusion section (Section 6).

2. Concepts of the new flexible MPIF process with multi-layer sheets

2.1. New flexible MPIF process

In the conventional MPIF (C-MPIF) process, a reconfigurable multi-point die is employed to replace the rigid die used in the TPIF process. As presented in Fig. 2(a), the multi-point pins used in the C-MPIF process are fixed in position without changing height from start to end. Each multi-point pin should be adjusted to the desired position before the forming operation. Boudhaouia et al. (2018) indicated that the sheet deformation in the C-MPIF process was identical to that in the TPIF process. In the new flexible MPIF (F-MPIF) process, as shown in Fig. 2 (b), a flexible multi-point die system has been developed. All multi-point pins are always in contact with the blank sheet. Therefore, the shape of the multi-point die should change in correspondence with the movements of the forming tool during the whole forming process.

Fig. 3(a) and (b) show the experimental setup for the conventional TPIF and the C-MPIF processes. A 4-axis milling machine needs to be used to carry out the testing. The X, Y and Z-axes of the CNC machine control the forming tool movement, while a lifting system is controlled by an extra A-axis to drive the blank holder. The blank sheet is rigidly clamped by the blank holder and moved downward along the four guiding pillars for the lifting system. The movements of the blank holder should be the same as the Z-axis motion of the forming tool.

The proposed new flexible multi-point die system is presented in Fig. 3(c). Apart from the main components used in the C-MPIF process, extra parts called the multi-point pin positioning limiters are used to control the vertical positions of the multi-point pin. The positioning limiters are essentially a number of cylindrical tubes with pre-defined heights, which are arranged into the designated positions according to the design profile at the initial state. These positioning limiters are used to stop the movement of the pins until they reach the designated positions. The basic concept of the F-MPIF process is that all multi-point pins support the blank sheet during the whole process. Therefore, each pin can move downward together with the blank holder before reaching the designated position.

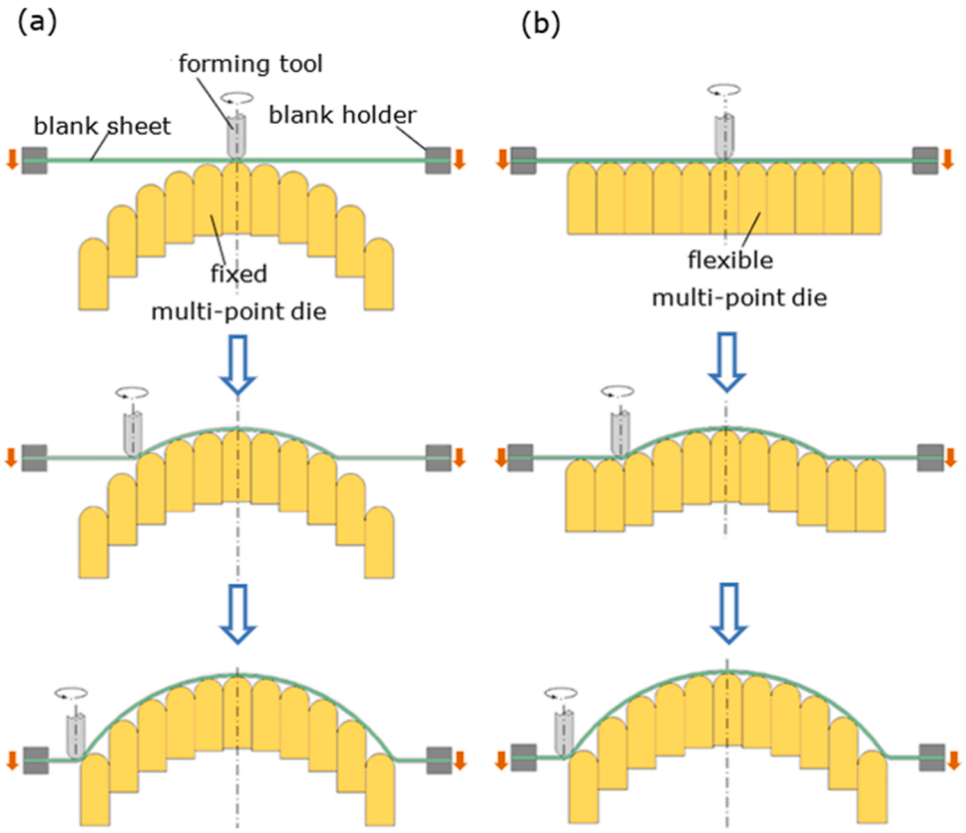

Fig. 2. Comparisons of forming principles between (a) C-MPIF, and (b) F-MPIF processes.

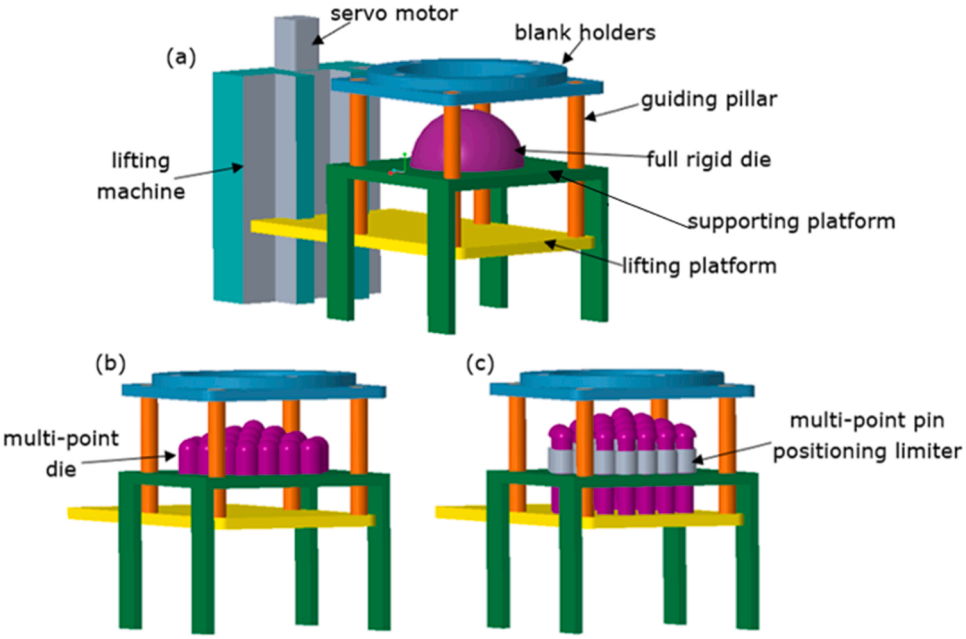

Fig. 3. Schematic illustration of experimental set-up for various forming processes: (a) conventional TPIF, (b) C-MPIF, and (c) F-MPIF processes.

Fig. 4 illustrates the operation of the new flexible multi-point pins during the forming process. In the beginning, all the pins are placed on the lifting platform and kept at the same height. During the forming operation, the lifting platform drives the multi-point pins and moves along with the blank holder, as shown in Fig. 3(c) and Fig. 4. When the first pin arrives at the designated position, it is separated from the lifting platform by the positioning limiter. The rest of the pins continue moving downwards with the lifting platform. In the end, all the pins arrive at the designated positions.

2.2. *New flexible MPIF process with multi-layer sheets*

Three sheets are employed in the conventional MPIF process with multi-layer sheets (C-MPIF-MLS), including an upper dummy sheet, a

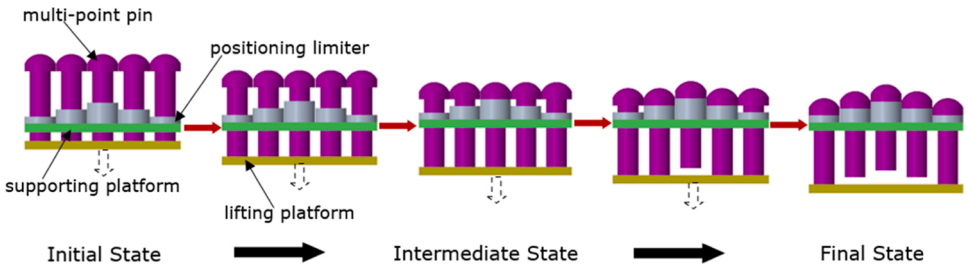

Fig. 4. Schematic illustration of the new flexible multi-point pins during forming process.

target blank sheet, and a polymer sheet. The upper dummy sheet is used to prevent the forming tool from contacting the target blank sheet directly, which helps enhance the surface quality of the formed sheet. When employing the multi-point die, dimples are inevitably created on the formed sheet. A piece of polymer sheet is placed above the multi-point die to minimise the dimpling effect. As the target blank sheet is sandwiched between the upper dummy and a polymer sheet, the target blank does not have to be rigidly clamped by the blank holders like the upper dummy sheet, which means the target blank sheet can be deformed without blank holder. Such a clamping condition of the target blank sheet gives the benefit of reduced sheet thinning during the new flexible MPIF process with multi-layer sheets (F-MPIF-MLS).

Fig. 5 illustrates the comparisons between the C-MPIF-MLS and F-MPIF-MLS processes. The main difference between these two forming processes is the arrangement of multi-point pins, whether these multi-point pins are fixed in position or flexible to allow synchronised motion with the ISF tool. The new F-MPIF-MLS process uses the flexible multi-point die, so the target blank sheet and polymer sheet can be supported and kept in contact with the flexible multi-point die until the end of the MPIF forming operation.

The following advantages are expected from the proposed new F-MPIF-MLS:

2.2.1. *Process flexibility*

The flexible multi-point die arrangement is reconfigurable, and the multi-point pins can be used to build a complicated 3D surface. Thus, it can improve the process flexibility as compared to the rigid dies used in the conventional TPIF process. The multi-point die can also reduce the cost and shorten the lead time by placing the simple positioning limiter as part of the supporting die system.

2.2.2. *Sheet thinning and thickness variation*

Chang and Chen (2022) observed that the maximum thinning region in the conventional ISF process was caused by the differences in the stress state between the bending region and the contacting areas of ISF under the effect of edge constraint. Thus, the authors proposed a flexible free ISF process to remove the impact from the edge constraint. Three pieces of sheet were employed when conducting the SPIF process, and

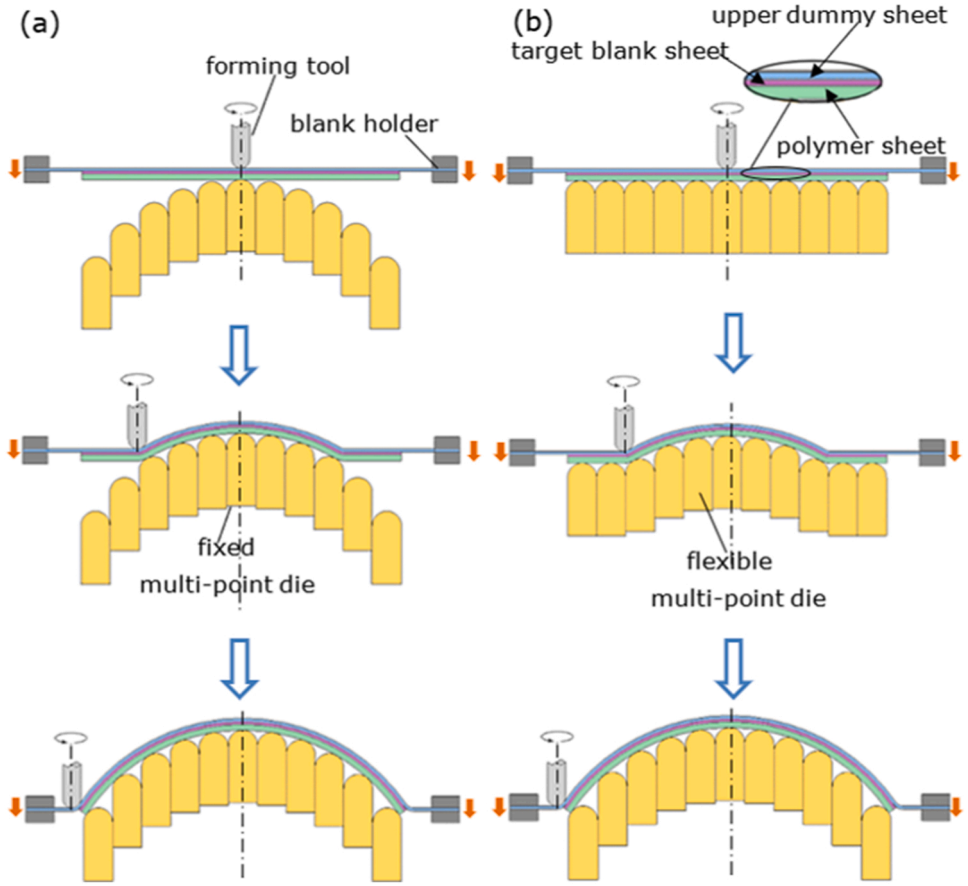

Fig. 5. Schematic illustrations: (a) C-MPIF-MLS and (b) new F-MPIF-MLS processes.

the target blank sheet could be deformed without blank holders. The results showed that a part without undesired thinning regions and a more homogeneous thickness could be produced by this flexible free ISF process. In this research, the proposed new F-MPIF-MLS process is similar to the flexible free ISF process. The target blank sheet can also be deformed without edge constraints, which is expected to reduce extreme sheet thinning and achieve a more uniform thickness distribution.

2.2.3. Surface quality

In the new F-MPIF-MLS process, a dummy sheet is implemented to avoid the forming tool being in direct contact with the target blank sheet. Therefore, the tool marks created from the ISF process can be significantly eliminated, which enhances the surface quality of the formed product.

3. Experimental testing

Fig. 6 shows the experimental setup for conducting testing. A 4-axis milling machine was used to conduct the experimental test. The forming tool was controlled by the X, Y, and Z axes of the milling machine, while an extra A-axis controlled the lifting machine to drive the blank holder to move vertically. The blank sheet was rigidly clamped by the blank holder and moved downward along four guiding pillars. The movement of the blank holder was synchronised with the forming tool in the Z-axis motion. The four guiding pillars were connected to the lifting platform, and the multi-point pins were also placed on the lifting platform. Thus, the multi-point pins and blank holders were moved downward with the lifting platform. The positioning limiters were made of cylindrical tubes with designated heights, which were used to stop the movements of the multi-point pins in their designed positions.

The forming tool used for all tests had a 10 mm diameter hemispherical head. These tests were carried out with a constant step size of 0.5 mm helical toolpath. The tool was rotation-free with a 200 mm/min feed rate. The blank sheet material was DC01 Steel, and the polymer sheet was polyurethane with a Shore A 90 hardness. Each multi-point pin had a hemispherical head of 20 mm in diameter. The multi-point pins were arranged in a hexagonal configuration, as presented in Fig. 7. In all tests, Rocol RTD Compound was used as lubricant applied to both the forming tool and the blank sheets.

4. Finite element modelling

ABAQUS/Explicit software was used to conduct FE simulations. The common components involved in the FE modelling of the C-MPIF, F-MPIF, C-MPIF-MLS, and F-MPIF-MLS processes included the forming tool, a blank sheet, a polymer sheet, and multi-point pins, as presented in Fig. 8. The target blank sheet was partitioned into clamping and forming regions rather than using blank holders to reduce the computing time. In the C-MPIF-MLS and F-MPIF-MLS processes, two pieces of metal blank sheets were used. And the upper dummy sheet was partitioned into clamping and forming regions.

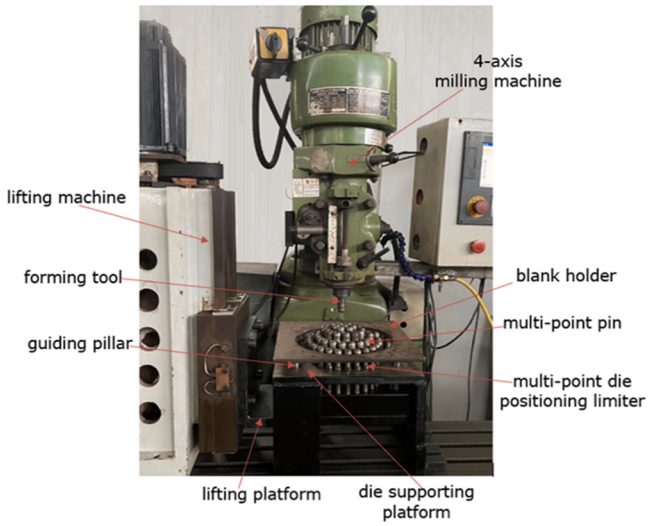

Fig. 6. Schematic illustration of experimental set-up.

Fig. 7. Multi point die set-up for experimental testing.

The forming tool and multi-point pins were modelled using rigid analytical shell elements. To smooth the curvature, the forming tool and multi-point dies were meshed with an element size of 0.5 mm. The DC01 Steel metal sheet and polyurethane sheet were modelled using 3D C3D8R-brick elements. The approximate size was 2 mm for the steel and polymer sheets, and three elements were considered along the through-thickness direction. DC01 Steel metal sheet with a 0.8 mm initial thickness was used as the blank sheet material. The mechanical properties and stress-strain curve used in the FE simulation were based on the tensile test. The flow stress curve of the DC01 steel sheet adopted in FE modelling is shown in Fig. 9.

A piece of polymer sheet was placed between the blank sheet and the multi-point die to prevent the dimpling effect. Concerning the material of the polymer sheet, Nourmohammadi et al. (2019) investigated the effects of using three different types of polymer sheets (natural rubber, silicon, and polyurethane) and the influence of a polyurethane sheet with different hardness on geometrical accuracy and sheet thinning in the MPIF process. The authors concluded that the differences among various materials were relatively small. However, the geometrical accuracy can be improved by increasing the hardness of the polyurethane sheet from Shore A 50–90. Boudhaouia et al. (2018) used a polyurethane sheet with a Shore A 65 hardness in their research on the MPIF process. Significant improvements in surface quality and geometrical accuracy were reported. According to these studies, polyurethane with a Shore A 90 hardness was used as the polymer sheet material in this analysis, and the thickness was 4 mm. The Mooney-Rivlin constitutive model was adopted to define the elastic properties of the polyurethane sheet. The Mooney-Rivlin constitutive model parameters and mechanical properties of the polyurethane sheet with Shore A 90 hardness are listed in Table 1.

Coulomb's friction law was used to define the interfacial behaviour between various components. The friction coefficient between the forming tool and blank sheet, the forming tool and upper dummy sheet, the upper dummy sheet and the target blank sheet was 0.05 (Duchêne et al., 2013). At the same time, the friction coefficients of 0.1 and 0.2 were defined between the blank sheet and polyurethane sheet, polyurethane sheet and multi-point pins, respectively (Boudhaouia et al., 2018; Nourmohammadi et al., 2019). A helical tool path with a constant step size of 0.5 mm and a feed rate of 200 mm/min was employed in this analysis. To save computation time, mass scaling was applied in this research. The mass scaling factor may lead to error or failure of the simulation due to the fact that kinetic energy can be raised if a large value of mass scaling is selected. While it may take long computation time if a small value of mass scaling is used. Therefore, a stable time

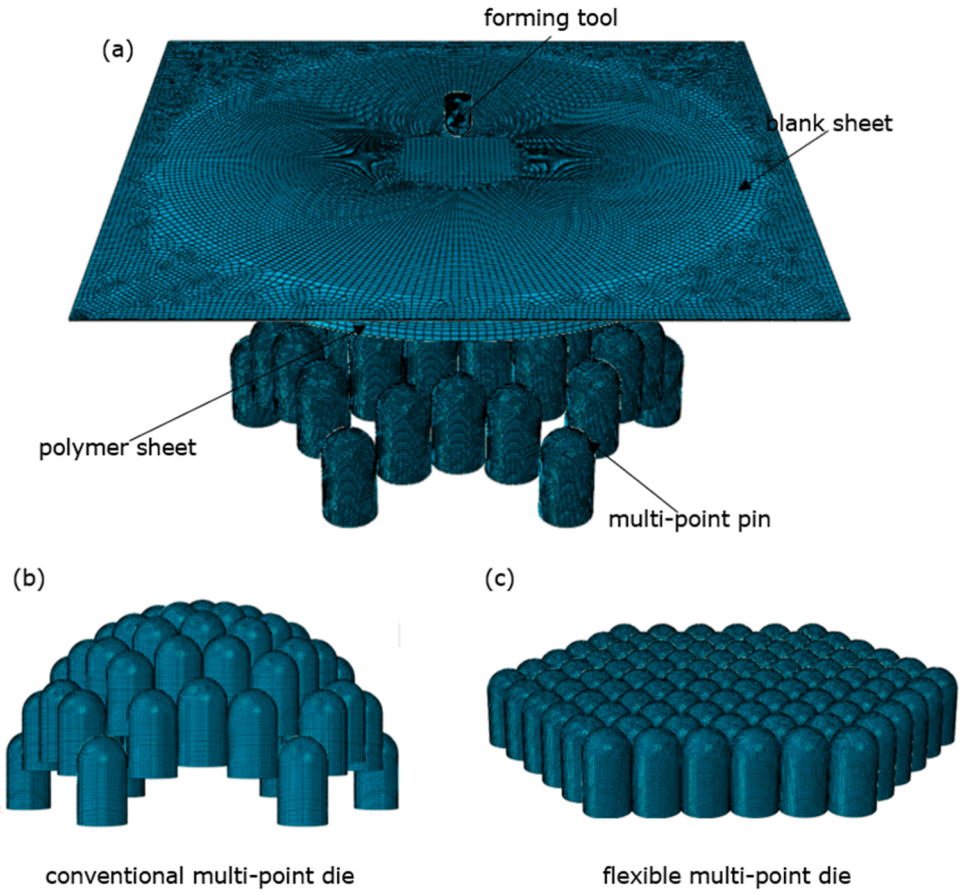

Fig. 8. FE model set-up for (a) C-MPIF process; and multi-point die initial set-up for (b) the conventional multi-point die, and (c) the new flexible multi-point die.

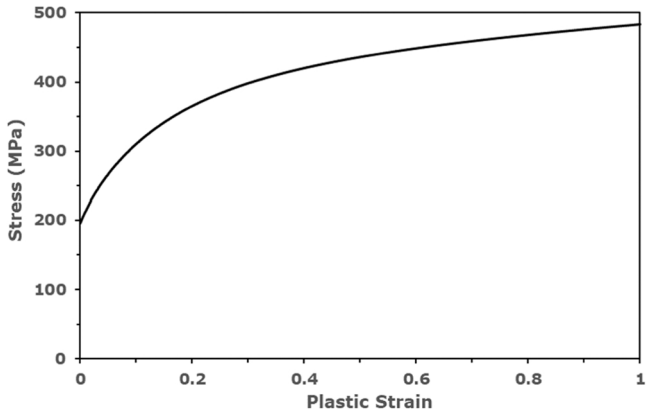

Fig. 9. DC01 steel sheet plastic stress-strain curve for FE modelling.

Table 1
Mooney-Rivlin constitutive model coefficients and mechanical properties of polyurethane with Shore A 90 hardness (Tolipov, 2019).

Hardness	C_{10}	C_{01}	Poisson's Ratio	Density
Shore A 90	0.861	0.354	0.499	$2e10^{-6}kg/mm^3$

increment of $2 \times 10^{-5}s$ was applied to ensure relative values between kinetic and internal energy are less than 0.4–10%.

In the C-MPIF process, each multi-point pin is positioned according to the designed profile and fixed in its initial position. The forming tool was controlled by its reference point and moved along the assigned tool path. To simplify the FE modelling, the blank sheet was partitioned into two regions: the deformation and the clamping regions. The displacement of the blank holder was applied to the clamping region. The blank sheet could only move vertically, and its motions should be identical to those of the forming tool in the Z direction. The edge boundary condition of the polyurethane sheet was set as free of constraint. In the case of the new F-MPIF process, except for the multi-point die, the boundary conditions of the forming tool, blank sheet, and polyurethane sheet were the same as in the C-MPIF FE modelling. The initial setup between the conventional and flexible multi-point dies is compared in Fig. 8(b) and (c). Each pin from the flexible multi-point die was controlled in real-time to keep contact with the blank sheet during the whole forming process. The flexible multi-point pins could only move downward, and the movements of the pins were synchronised with those of the blank holder (tool path in the Z direction) until they arrived at the designed positions. The final positions for all the pins were generated according to the desired profile. When employing multi-layer sheets, the movements were applied to the upper dummy sheet clamped region, which allowed the sheet to move vertically and to keep the same speed as the forming tool in the Z-direction. The target blank sheet and polyurethane sheet were placed between the multi-point die and the upper dummy sheet, and these two sheets were both deformed without clamping, so there was no edge constraint for these two sheets.

5. Results and discussion

In validate the developed forming processes, comparisons are made using the C-MPIF and the proposed F-MPIF and F-MPIF-MLS processes to form a symmetrical dome shape with a 53.4° draw angle. The experimental testing and FE results are discussed in this section.

5.1. Conventional MPIF and new flexible MPIF processes

A detailed comparison of material deformations between the C-MPIF and F-MPIF processes is conducted to demonstrate the new flexible multi-point die system. Fig. 10 presents the test results obtained from the C-MPIF and F-MPIF processes. There are no obvious dimples in the formed parts, although some slight dimpling marks are observed in the central regions. Increasing the hardness and thickness of the polymer sheet are considered options for future investigation to suppress the dimples completely.

5.1.1. Strain and stress distributions

Fig. 11 illustrates the distributions of equivalent plastic strain (PEEQ) and von Mises stress of the parts before unclamping from the blank holders, obtained from FE simulations for both the C-MPIF and F-MPIF processes. It can be found that the strain and stress distributions in the formed dome shape produced by these two forming processes are similar to each other.

The maximum strain and stress concentrations are both presented at a certain distance (about 65 mm) from the centre of the dome shape. The strain and stress distributions show low values at the centre of the parts and increase progressively to reach the maximum value, which is located at the maximum wall angle. The differences between the maximum equivalent plastic strains and von Mises stresses obtained in the two formed parts are 4.7% and 0.08%, respectively. It can be stated that the material deformations between the C-MPIF and F-MPIF processes are similar.

5.1.2. Thickness variations

The sheet thickness distributions of the dome shape along the meridional cross-section from FE simulation and testing are shown in Fig. 12. In both cases, the minimum thickness is observed between the deformed and transition regions, where the maximum draw angle is achieved. The trends in thickness distribution between these two forming processes are the same. The sheet thickness decreases gradually in the radial direction with the increase in wall angle, which is in good correlation with the strain distributions obtained by FE simulations, as shown in Fig. 11 (a) and (b).

According to Fig. 12, the FE models accurately predict the sheet thickness distributions. The location of the minimum thickness predicted by FE simulations corresponds well with the experimental results. With an initial thickness of 0.8 mm, the measured minimum thickness is 0.6 mm, which is a 25% reduction for both the C-MPIF and F-MPIF processes. It can be concluded that the tendency of the sheet thickness variations in the F-MPIF process is identical to the C-MPIF process.

5.1.3. Geometrical accuracy

To evaluate the geometrical accuracy, the experimental and FE predicted profiles of the formed part are compared with the designed CAD model along the meridional cross-section, as shown in Fig. 13. In this study, a 4 mm thick polyurethane sheet with a Shore A 90 hardness was placed between the blank sheet and the multi-point die to overcome the dimpling defect. Due to the characteristics of the hyperelastic polymer material, the amount of elastic compression could lead to deviations between the formed part and the desired profile. The maximum geometrical inaccuracy is found in the central region for both forming processes.

Geometrical deviations are used to capture the amount of dimensional inaccuracy. Fig. 14 illustrates the comparison of geometrical deviations of the formed dome shape obtained from the C-MPIF and F-MPIF processes. A similarity between experimental and simulation results can be observed. The maximum profile inaccuracies of the predicted results as compared to experimental values are 8.4% and 8.6% for the C-MPIF and F-MPIF processes, respectively. Profile deviations from the desired shape occur from 10 mm to the centre, with a maximum reaching 1.8 mm for both forming processes. These inaccuracies could be attributed to the amount of compression in the polymer sheet, which can be improved by reorganising the multi-point pin positions, optimising the tool path, and increasing the thickness and hardness of the polymer sheet. It could be concluded that the same amounts of geometrical inaccuracies were obtained from both the C-MPIF and F-MPIF processes, with a difference of less than 0.2%.

In conclusion, according to the experimental testing and FE simulation results, the material flow and the sheet deformations in these two processes were the same. The blank sheets were rigidly clamped by the blank holders in both forming processes. As a result, the implementation of the flexible multi-point die did not affect the material deformation significantly different from that of the C-MPIF process.

5.2. Conventional MPIF with multi-layer sheets and new flexible MPIF processes with multi-layer sheets

The main difference between the C-MPIF-MLS and F-MPIF-MLS processes is the arrangement of the multi-point die, as presented in Fig. 5. Due to the use of the flexible multi-point die, the target blank sheet and polymer sheet can be supported and kept in contact with flexible multi-point pins during the whole forming operation in the new F-MPIF-MLS process.

Fig. 15 shows the comparisons of FE predicted and experimental results for the parts produced by the C-MPIF-MLS and F-MPIF-MLS processes. The experimental results are consistent with the FE simulation results. The flange of the part produced by using a fixed multi-point die is visibly wrinkled, which failed to achieve the designed dome shape. On the contrary, the new F-MPIF-MLS process successfully produced the desired dome shape. In addition, compared to the C-MPIF-MLS process, a more uniform strain distribution is obtained when using the flexible multi-point die to replace the conventional multi-point die, as presented in Fig. 15 (a) and (b).

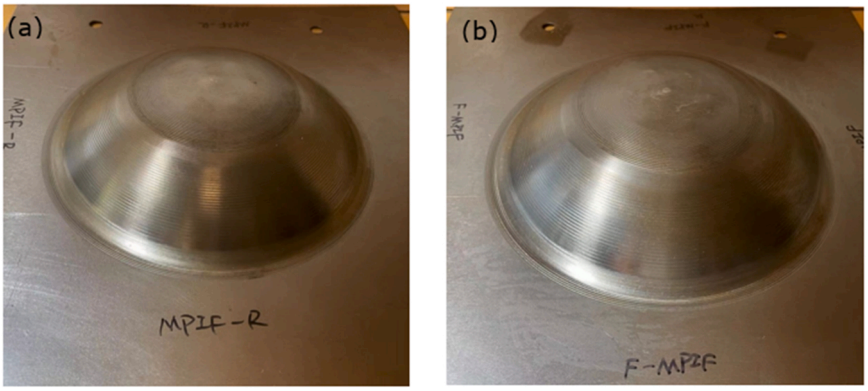

Fig. 10. Experimental results produced by (a) C-MPIF and (b) F-MPIF processes.

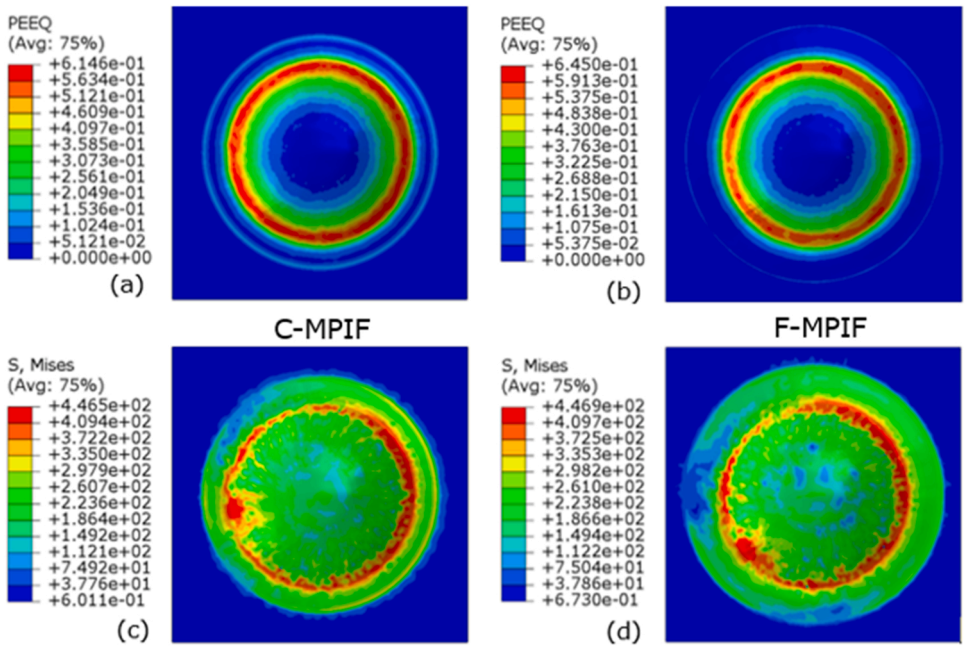

Fig. 11. Equivalent plastic strain and von Mises stress distributions produced by: (a) (c) C-MPIF and (b) (d) F-MPIF processes.

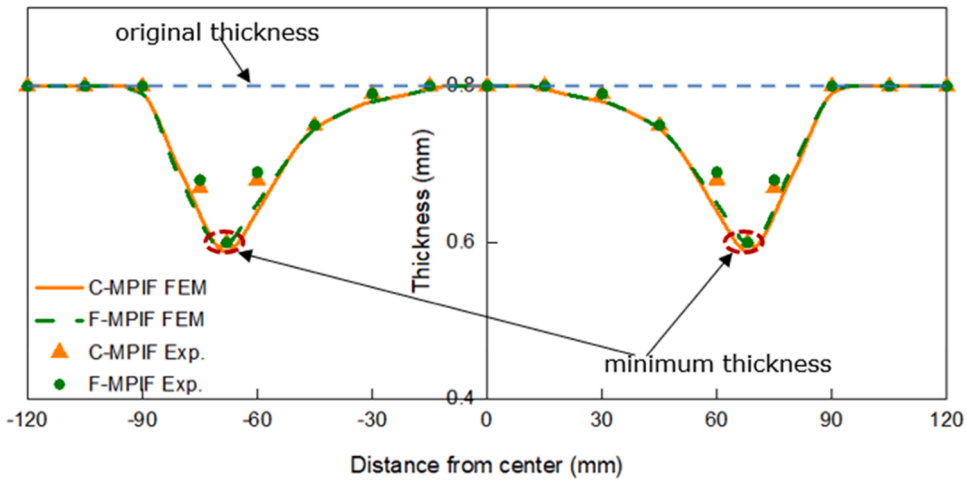

Fig. 12. Comparisons of sheet thickness distributions along the meridional cross-section between C-MPIF and F-MPIF processes.

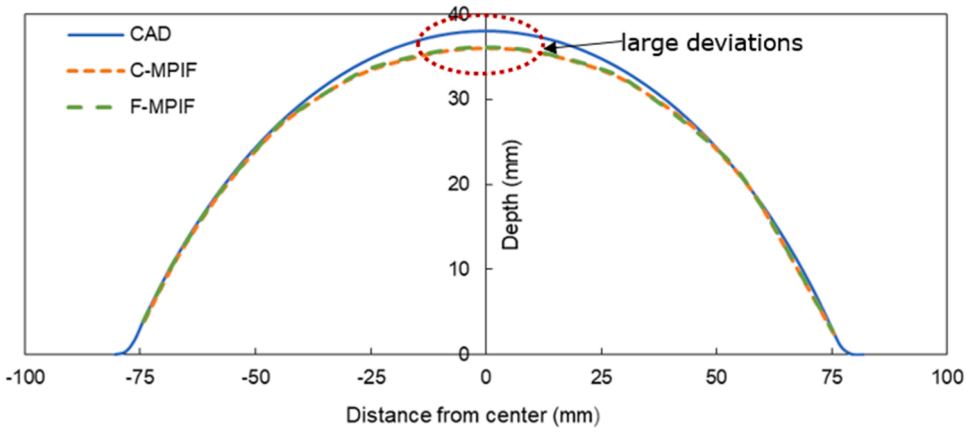

Fig. 13. Comparisons of FE predicted and experimental profiles of the formed parts along meridional cross-section with designed CAD model.

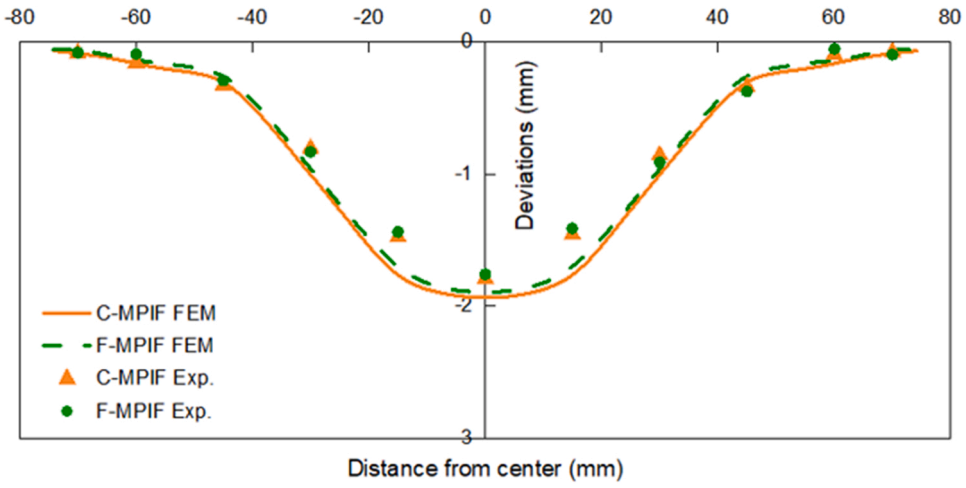

Fig. 14. Comparison of geometrical deviations between the C-MPIF and F-MPIF processes.

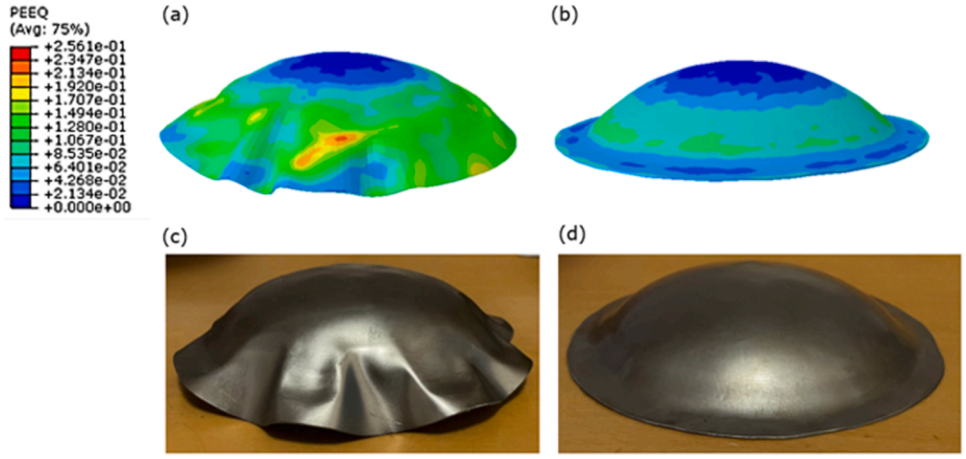

Fig. 15. Comparisons of FE predicted, and experimental testing results of the parts produced by (a) (c) C-MPIF-MLS and (b) (d) new F-MPIF-MLS processes.

Fig. 16 presents a comparison between the C-MPIF-MLS and F-MPIF-MLS processes obtained from the FE simulations. Using Δ to represent the total percentage of prescribed deformation. Prominent flange wrinkles occur in the case of the C-MPIF-MLS process when the amount of deformation Δ was 20% of the defined forming depth, as shown in Fig. 16 (a). The flange wrinkling is due to the sheet instability under circumferential compressive stress. When the ratio of the circumferential compressive stress and the radial tensile stress reaches a critical value, and there is no normal pressure to suppress it, wrinkles appear and generate out-of-plane deformation in the form of wave-like perturbations (Altan and Tekkaya, 2012). Fig. 16 (b) shows that no wrinkles occur on the blank sheet produced by the new F-MPIF-MLS process.

In capture and analyse the flange wrinkles, 32 points on the outer edge of the blank sheet are picked, as shown in Fig. 17 (a). In Fig. 17 (b), the Z-coordinates represent the picked point positions along the Z-axis. Once wrinkling occurs, the Z-coordinate values of the selected points present a waveform distribution. A noticeable wave-like curve is obtained in the case of the C-MPIF-MLS process. This can be explained by the large gap between the sheet and the supporting conventional multi-point die during the forming operation. However, no flange wrinkling is observed in the formed dome shape produced by the new F-MPIF-MLS process. This indicates that the proposed flexible multi-point die can effectively suppress the plastic instabilities and wrinkling on the edge of the blank sheet. This wrinkling suppression is attributed to the constant contact between the flexible multi-point die and the target blank sheet during the whole forming process. The upper dummy sheet and flexible multi-point die offer compression to the blank sheet, which delays the onset of circumferential compressive instabilities to prevent the wrinkling defect.

The flange wrinkling is caused by the circumferential compression instability of the flange region. To study the wrinkling behaviour, the circumferential stress distributions at 20% of the process between the C-MPIF-MLS and F-MPIF-MLS processes are compared, as shown in Fig. 18. High circumferential compressive stress is concentrated in the highlighted flange wrinkling regions, as shown in Fig. 18 (a). According to Fig. 17 (b) and Fig. 18 (a), the crest of the wrinkle wave corresponds to the low compressive or tensile stress region, while the trough of the wrinkle wave corresponds to the high compressive stress region. These results are in general agreement with the findings by Chen et al. (2021). In addition, the regions in contact with the forming tool may also result in considerable circumferential compressive stress. However, if the circumferential compressive stress does not exceed its critical value against wrinkling, no wrinkling would occur. As shown in Fig. 18 (b), a more uniform circumferential stress distribution is obtained in the flange region when employing a flexible multi-point die. And only the forming tool contact region is under high circumferential compressive stress.

To investigate the stress variations between the C-MPIF-MLS and F-MPIF-MLS processes, location A is picked from the significant wrinkling region to conduct the analysis, as shown in Fig. 16. Fig. 19 presents the

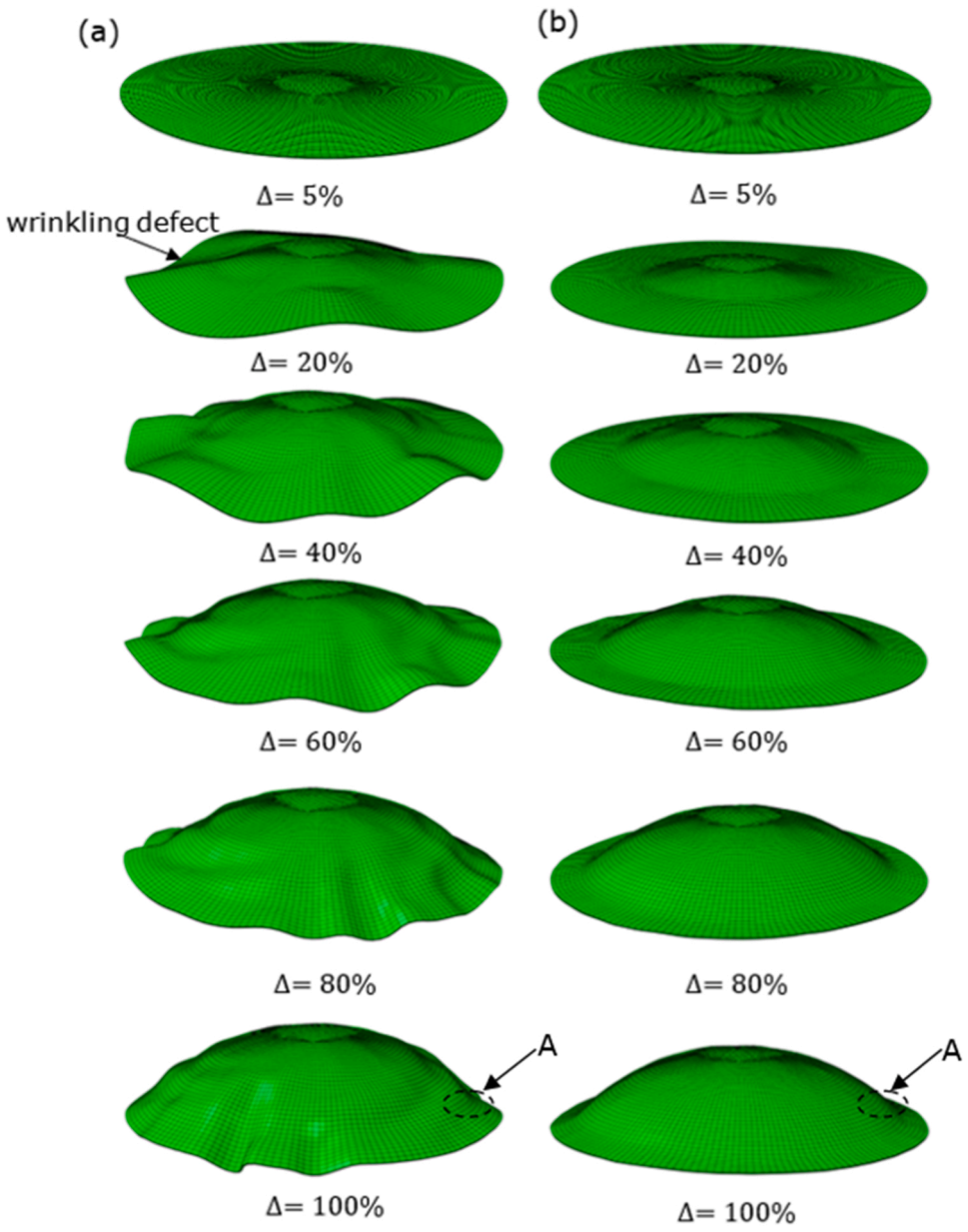

Fig. 16. Comparisons of deforming process between the (a) C-MPIF-MLS and (b) new F-MPIF-MLS processes.

evolutions of stress components in the local coordinate system of location A against the forming time. The stress along the inclined wall and perpendicular to the forming tool motion is defined as meridional stress σ_ϕ, the circumferential stress σ_θ is along the forming tool motion, and through-thickness stress is defined as σ_t, respectively. When using the conventional multi-point die, it can be found that the circumferential stress σ_θ is compressive during the whole forming process, and the compression instability along the circumferential direction results in a wrinkling defect. When the forming tool moves to location A, the circumferential stress σ_θ turns to compressive when using the flexible multi-point die. But no wrinkles are observed. Because the flexible multi-point pins keep direct contact with the blank sheet, the through-thickness stress σ_t is higher than that when using the conventional multi-point die, which provides the normal pressure to suppress wrinkling. In addition, the meridional stress σ_ϕ in the new F-MPIF-MLS process is larger than that in the C-MPIF-MLS process, which is also caused by the extra compressive stress of the flexible multi-point die on the target blank sheet.

It can be concluded that the implementation of the proposed new flexible multi-point die system can effectively suppress the wrinkling defect in the new F-MPIF-MLS. As compared to the conventional fixed multi-point die, more uniform strain and stress distributions can be obtained.

5.3. Conventional MPIF process and new flexible MPIF process with multi-layer sheets

To further validate the proposed new F-MPIF-MLS process, a comparative investigation of material deformation, strain and stress distributions, thickness variations, and geometrical accuracy between the C-MPIF and F-MPIF-MLS processes was carried out in this section.

In the new F-MPIF-MLS process, a dummy sheet was placed above the target blank sheet. Thus, the forming tool was in direct contact with the target blank sheet. Better surface quality was achieved by the new F-MPIF-MLS process in comparison with the C-MPIF formed part, as presented in Fig. 10 (a) and Fig. 15 (d).

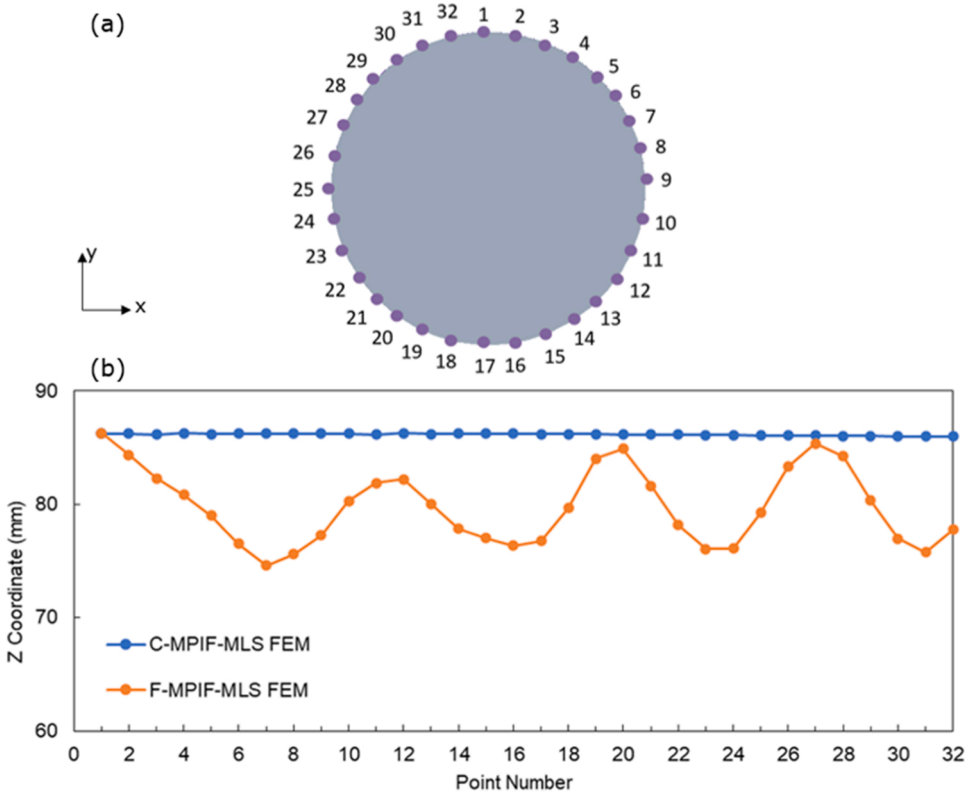

Fig. 17. Wrinkling defect at the stage of 20% of the process: (a) the positions of selected 16 points, and (b) the Z coordinate values of the selected points.

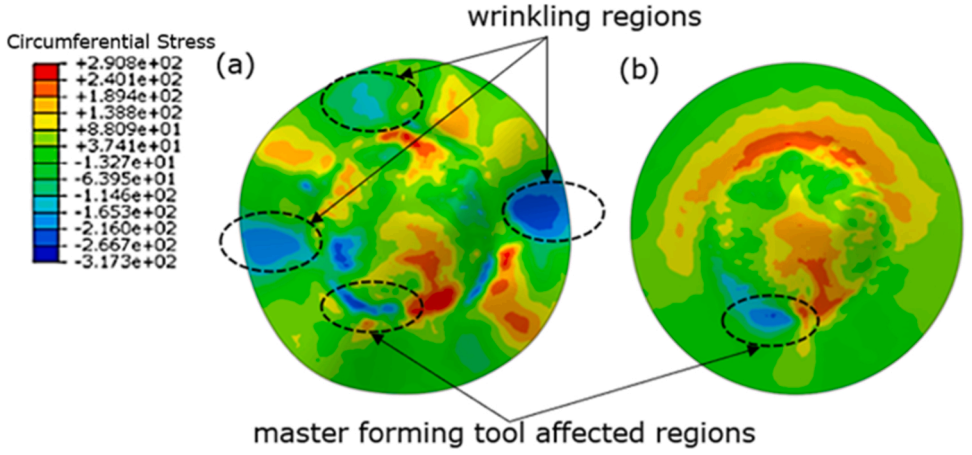

Fig. 18. Circumferential stress distributions of the parts produced by the (a) C-MPIF-MLS, and (b) new F-MPIF-MLS at the 20% of the process.

5.3.1. Strain distributions

Fig. 20 (a) and (b) show the comparisons of equivalent plastic strain distributions between the C-MPIF process and the new F-MPIF-MLS process obtained from FE simulations. In both cases, the maximum PEEQ occurred in the largest wall-angle region. The maximum PEEQ in the C-MPIF process was almost three times higher than that produced by the new F-MPIF-MLS process. The strain distributions between these two forming processes were similar, starting from low values at the centre of the parts and increasing with the draw angles. However, more uniform strain distributions could be generated by the new F-MPIF-MLS process in comparison with the C-MPIF process.

Fig. 20 (c) shows the strain components in the local coordinate system along the dotted paths. The evolutions of meridional strain (ε_ϕ), circumferential strain (ε_θ), and through-thickness strain (ε_t) were compared between the C-MPIF and the new F-MPIF-MLS processes. In the case of the C-MPIF process, it is observed that although the circumferential strain does not attain an ideal zero value, the meridional and through-thickness strains are larger than the circumferential strain. This finding aligns with the results obtained by Zhu and Ou (2023), suggesting a general plane strain condition with elongation, the meridional direction and compensated for in the thickness direction (Martins et al., 2008; Fang et al., 2014). It is also clear that in the case of the new F-MPIF-MLS process, more uniform material deformation is achieved through smaller amounts of meridional, circumferential and thickness strain variations.

5.3.2. Thickness variations

The predicted and measured results of thickness variations are

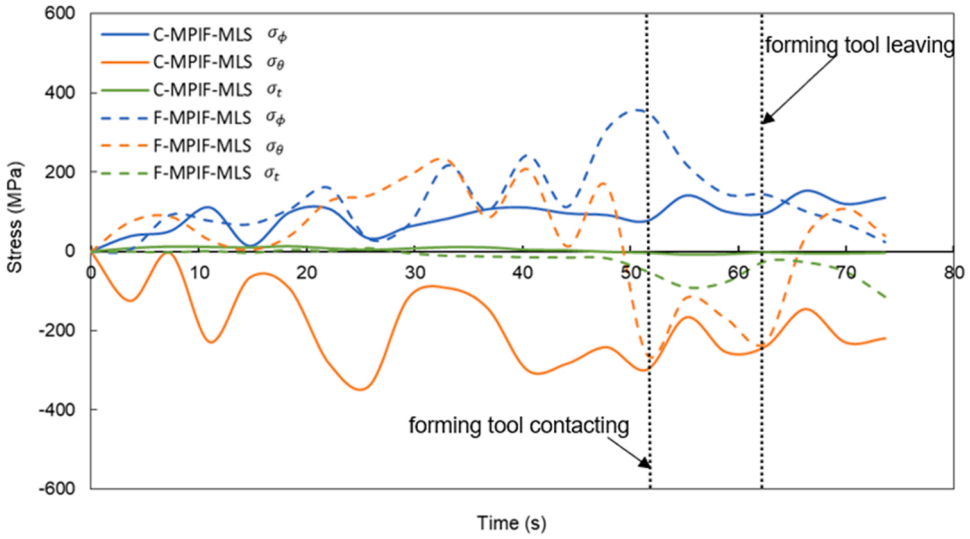

Fig. 19. Comparisons of stress components of location A between the C-MPIF-MLS and new F-MPIF-MLS processes.

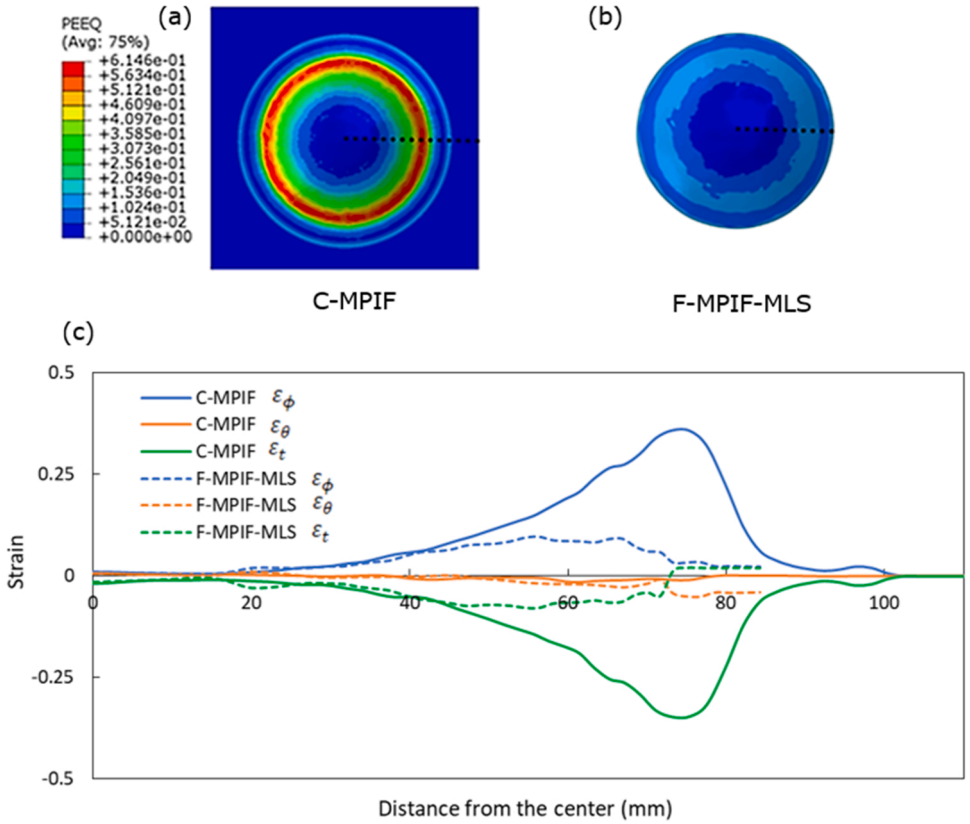

Fig. 20. Equivalent plastic equivalent strain distributions of the parts produced by (a) C-MPIF, and (b) new F-MPIF-MLS processes; (c) strain components distributions along dotted paths.

compared in Fig. 21. Similar results were obtained from both FE simulation and measurement. The minimum thickness is 0.6 mm and 0.76 mm from experimental testing, which are very close to the FE simulation results of 0.596 mm and 0.748 mm for the C-MPIF and new F-MPIF-MLS processes, respectively. The thickness variation trends are similar to the strain distributions, as shown in Fig. 20. In both cases, the sheet thickness decreases gradually in the radial direction with the increase in draw angle. Maximum thickness reduction occurs in the region of the largest draw angle. However, a part with a more uniform thickness distribution can be produced by the new F-MPIF-MLS process, and the thickness of most regions is the same as the initial thickness of 0.8 mm. Moreover, both predicted and measured results show that the flange region thickness in the F-MPIF-MLS process formed parts is increased from 0.8 mm to 0.83 mm, which corroborates the sudden change in through thickness strain observed in Fig. 20 (c).

As shown in Fig. 21, the measured minimum thickness of the part produced by the new F-MPIF-MLS process was 0.76 mm, a 5% reduction from the initial thickness. The measured minimum thickness for the C-MPIF process part is 0.6 mm, a thickness reduction of 25%. It can be concluded that much reduced sheet thinning is achieved by using the

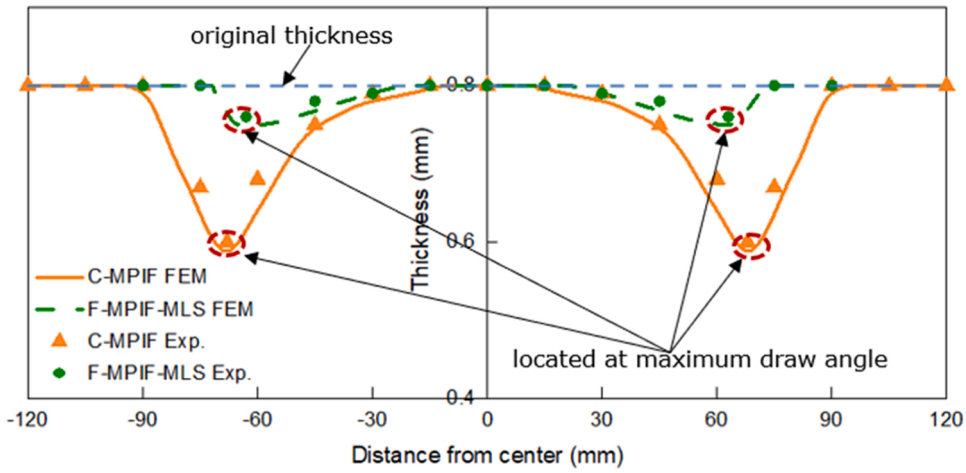

Fig. 21. Thickness distribution along the meridional cross section for the parts produced by C-MPIF and new F-MPIF-MLS processes.

new F-MPIF-MLS process. And the thickness distribution is more homogenous than the part produced by the C-MPIF process. This is because the edge of the target blank sheet is free of constraints in the F-MPIF-MLS process.

5.4. Geometrical accuracy

Based on the FE simulation and experimental findings, Fig. 22 illustrates the comparison of geometrical deviations between the formed parts produced by the C-MPIF and the F-MPIF-MLS processes. In terms of geometrical accuracy, the experimental and simulation results were similar. The largest deviations in predicted results relative to measured values are observed to be 7.2% and 8.9% for the C-MPIF process and F-MPIF-MLS process, respectively. And the maximum deviations occur in the central regions, with a measured value of 1.8 mm for both cases. This geometrical inaccuracy may be due to the use of the polyurethane sheet. The overall geometrical accuracies of the C-MPIF and the F-MPIF-MLS processes are in good agreement. The differences between the dimensional deviations of these two parts are less than 0.62%.

6. Conclusions

In this research, the proposed new F-MPIF-MLS process and its benefits were demonstrated. In the new F-MPIF process, a group of flexible multi-point pins is used to replace the rigid die, which ensure that all multi-point pins are in constant contact with the blank sheet during the forming process. Based on this concept, the new F-MPIF-MLS process is developed. Comparative investigations into the C-MPIF, F-MPIF, C-MPIF-MLS and F-MPIF-MLS processes are conducted through experimental testing and FE simulations. Conclusions can be drawn as follows:

1) No significant improvements were obtained when using the flexible multi-point die to replace the conventional fixed multi-point die in the MPIF process. Even though the blank sheet was supported by the multi-point die all the time, the material flow and the sheet deformations in the F-MPIF process are similar to the C-MPIF process.
2) When employing multi-layer sheets with the target blank sheet placed between the upper dummy sheet and the polymer sheet and deformed without clamping, the implementation of the flexible multi-point die presented notable benefits in forming the dome shape without distinct wrinkling by using the new F-MPIF-MLS process. This is in contrast with the C-MPIF-MLS process, in which a significant amount of flange wrinkling was observed, and it failed to create the designed dome shape.
3) The new F-MPIF-MLS process led to a considerable reduction in material thinning due to the relaxed edge constraints of the blank sheet sandwiched between the upper dummy and polyurethane sheet. When producing the dome shape, the maximum thickness reduction was significantly reduced from 35% to 5% from the C-MPIF process to the F-MPIF-MLS process.

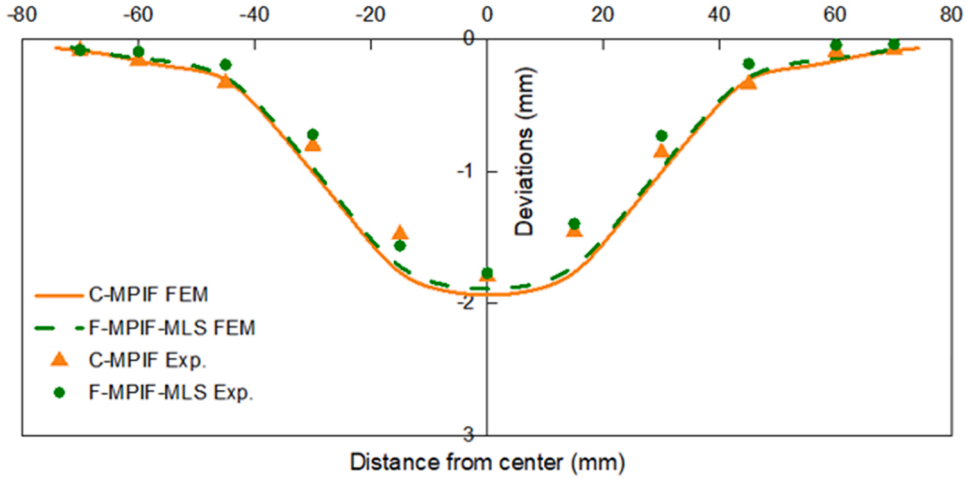

Fig. 22. Geometrical deviations between the C-MPIF and new F-MPIF-MLS processes.

4) The proposed new F-MPIF-MLS process showed no enhancement in geometrical accuracy. Dimensional deviations caused by the polymer sheet and dimples were still an issue with the new flexible MPIF forming process. Thus, future work needs to focus on the generation of a new buffer pad to replace the polymer sheet for improvement.

CRediT authorship contribution statement

Xuelei Zhao: Conceptualization, Methodology, Investigation, Data curation, Formal analysis, Software, Validation, Writing – original draft. **Hengan Ou**: Conceptualization, Methodology, Validation, Writing – review & editing, Supervision, Funding acquisition.

Declaration of Competing Interest

The authors declare that they have no known competing financial interests or personal relationships that could have appeared to influence the work reported in this paper.

Data Availability

We can share relevant data with the institutional approval.

Acknowledgements

This work was partly supported by the Engineering and Physical Sciences Research Council [grant number EP/W010089/1].

References

Altan, T., Tekkaya, A.E., 2012. Sheet metal forming: fundamentals. Asm International, pp. 120–127.
Ambrogio, G., Cozza, V., Filice, L., Micari, F., 2007. An analytical model for improving precision in single point incremental forming. J. Mater. Process. Technol. 191, 92–95.
Attanasio, A., Ceretti, E., Giardini, C., Mazzoni, L., 2008. Asymmetric two points incremental forming: improving surface quality and geometric accuracy by tool path optimization. J. Mater. Process. Technol. 197, 59–67.
Bagudanch, I., Sabater, M., Garcia-Romeu, M.L., 2017. Single point versus two point incremental forming of thermoplastic materials. Adv. Mater. Process. Technol. 3, 135–144.
Boudhaouia, S., Gahbiche, M.A., Ayed, Y., Giraud, E., Ben Salem, W., Dal Santo, P., 2018. Experimental and numerical study of a new hybrid process: multi-point incremental forming (MPIF). Int. J. Mater. Form. 11, 815–827.
Cai, Z.Y., Wang, S.H., Li, M.Z., 2008. Numerical investigation of multi-point forming process for sheet metal: Wrinkling, dimpling and springback. Int. J. Adv. Manuf. Technol. 37, 927–936.
Chang, Z., Chen, J., 2020. Investigations on the deformation mechanism of a novel three-sheet incremental forming. J. Mater. Process. Technol. 281, 1–10.
Chang, Z., Chen, J., 2022. Investigations on the forming characteristics of a novel flexible incremental sheet forming method for low-ductility metals at room temperature. J. Mater. Process. Technol. 301, 1–10.
Chen, S., Zhan, M., Gao, P., Ma, F., Zhang, H., 2021. A new robust theoretical prediction model for flange wrinkling in conventional spinning. J. Mater. Process. Technol. 288, 1–12.
Duchêne, L., Guzmán, C.F., Behera, A.K., Duflou, J.R., Habraken, A.M., 2013. Numerical simulation of a pyramid steel sheet formed by single point incremental forming using solid-shell finite elements. In: Key Engineering Materials, 549. Trans Tech Publ, pp. 180–188.
Duflou, J.R., Habraken, A.-M., Cao, J., Malhotra, R., Bambach, M., Adams, D., Vanhove, H., Mohammadi, A., Jeswiet, J., 2018. Single point incremental forming: state-of-the-art and prospects. Int. J. Mater. Form. 11, 743–773.
Erhu, Q., Mingzhe, L., Rui, L., Mingyang, C., Jianlei, L., 2018. Research on formability in multi-point forming with different elastic pads. Int. J. Adv. Manuf. Technol. 98, 1887–1901.
Fang, Y., Lu, B., Chen, J., Xu, D., Ou, H., 2014. Analytical and experimental investigations on deformation mechanism and fracture behavior in single point incremental forming. J. Mater. Process. Technol. 214, 1503–1515.
Jeswiet, J., Micari, F., Hirt, G., Bramley, A., Duflou, J., Allwood, J., 2005. Asymmetric single point incremental forming of sheet metal. CIRP Ann. 54, 88–114.
Kumar, A., Gulati, V., Kumar, P., Singh, H., 2019. Forming force in incremental sheet forming: a comparative analysis of the state of the art. J. Braz. Soc. Mech. Sci. Eng. 41, 1–45.
Lasunon, O., Knight, W., 2007. Comparative investigation of single-point and double-point incremental sheet metal forming processes. Proc. Inst. Mech. Eng., Part B: J. Eng. Manuf. 221, 1725–1732.
Li, M., Cai, Z., Liu, C., 2007. Flexible manufacturing of sheet metal parts based on digitized-die. Robot. Comput. -Integr. Manuf. 23, 107–115.
Li, X., Li, M.Z., Liu, C., Cai, Z.Y., 2009. Principle and simulation study on multi point-single point incremental combined forming for sheet metal. In: Materials Science Forum, 626. Trans Tech Publ, pp. 273–278.
Liu, Y., Li, M., Ju, F., 2017. Research on the process of flexible blank holder in multi-point forming for spherical surface parts. Int. J. Adv. Manuf. Technol. 89, 2315–2322.
Lu, B., Zhang, H., Xu, D., Chen, J., 2014. A hybrid flexible sheet forming approach towards uniform thickness distribution. Procedia CIRP 18, 244–249.
Lu, H., Kearney, M., Wang, C., Liu, S., Meehan, P.A., 2017. Part accuracy improvement in two point incremental forming with a partial die using a model predictive control algorithm. Precis. Eng. 49, 179–188.
Martins, P., Bay, N., Skjødt, M., Silva, M., 2008. Theory of single point incremental forming. CIRP Ann. 57, 247–252.
Nakajima, N., 1969. A newly developed technique to fabricate complicated dies and electrodes with wires. Bull. JSME 12, 1546–1554.
Nourmohammadi, A.A., Elyasi, M., Mirnia, M.J., 2019. Flexibility improvement in two-point incremental forming by implementing multi-point die. Int. J. Adv. Manuf. Technol. 102, 2933–2952.
Peng, W., Ou, H., 2023. Deformation mechanisms and fracture in tension under cyclic bending plus compression, single point and double-sided incremental sheet forming processes. Int. J. Mach. Tools Manuf. 184, 1–21.
Peng, W., Ou, H., Becker, A., 2019. Double-sided incremental forming: a review. J. Manuf. Sci. Eng. 141, 1–12.
Reddy, N.V., Lingam, R., Cao, J., 2015. Incremental metal forming processes in manufacturing. Handbook of manufacturing engineering and technology. Springer,, pp. 411–452.
Silva, M., Martins, P., 2013. Two-point incremental forming with partial die: theory and experimentation. J. Mater. Eng. Perform. 22, 1018–1027.
Tolipov, A., 2019. Multi-point forming utilising novel elastic cushion designs. University of Birmingham.
von Finckenstein, (1995). "An approach for flexibilization of the sheet metal part production." Production Engineering.
Xu, P., Li, X., Feng, F., Li, X., Yang, Y., 2023. Experimental and numerical studies on two-point incremental forming of woven fabric composite sheet. J. Manuf. Process. 85, 205–215.
Zhang, H., Lu, B., Chen, J., Feng, S., Li, Z., Long, H., 2017. Thickness control in a new flexible hybrid incremental sheet forming process. Proc. Inst. Mech. Eng., Part B: J. Eng. Manuf. 231, 779–791.
Zhang, Q.-F., Cai, Z.-Y., Zhang, Y., Li, M.-Z., 2013. Springback compensation method for doubly curved plate in multi-point forming. Mater. Des. 47, 377–385.
Zhu, H., Ou, H., 2023. A new analytical model for force prediction in incremental sheet forming. J. Mater. Process. Technol. 318, 1–24.